Jan Hrabě

Fast optical tracking of diffusion in time-dependent environment of brain extracellular space
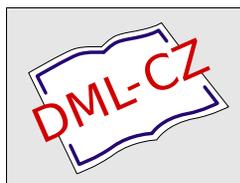
FAST OPTICAL TRACKING OF DIFFUSION IN TIME-DEPENDENT ENVIRONMENT OF BRAIN EXTRACELLULAR SPACE

Jan Hrabě[1,2]

[1] Center for Advanced Brain Imaging, Nathan S. Kline Institute
140 Old Orangeburg Road, Orangeburg, NY 10962, USA
hrabe@nki.rfmh.org
[2] Department of Cell Biology, SUNY Downstate Medical Center
Brooklyn, NY 11203, USA

Abstract

An improved version of the Integrative Optical Imaging (IOI) method for diffusion measurements in a geometrically complex environment of the brain extracellular space has been developed. We present a theory for this Fast Optical Tracking Of Diffusion (FOTOD) which incorporates a time-dependent effective diffusion coefficient in homogeneous anisotropic media with time-dependent nonspecific linear clearance. FOTOD can be used to measure rapid changes in extracellular diffusion permeability that occur, e.g., during brain insults. The achievable time resolution is approximately one second, a ten fold improvement compared to the traditional IOI method.

1. Introduction

Brain cells (neurons and glia) are surrounded by an extracellular space (ECS) that facilitates diffusion transport of neuroactive substances, nutrients, metabolites and therapeutic agents. Our knowledge about the ECS in living brain tissue has largely been deduced from studying diffusion of extracellular marker molecules [2]. The ECS is a geometrically complex porous environment [4] characterized by two basic properties: volume fraction α and diffusion permeability θ, see [1]. Volume fraction is the proportion of brain tissue volume occupied by the ECS and primarily governs concentration of molecules released into the ECS. Diffusion permeability, a ratio of the effective diffusion coefficient to its value in an obstacle-free medium, describes how much a diffusion-mediated process is slowed down in the ECS by obstacles represented by the cells and their various appendages. One additional parameter, κ, accounts for small nonspecific clearance proportional to the concentration. It describes nonspecific loss of marker molecules over time, e.g., into blood stream.

We will address the physiologically important situation where the diffusion permeability depends on time, as is observed during brain insults, e.g., following a stroke.

Our assumption is that the brain ECS environment remains homogeneous, that is, the time-dependent changes are everywhere the same. However, we do allow the medium to be anisotropic, as typified by white matter fiber tracts.

The diffusion experiment consists of releasing a small amount of a fluorescent substance into the ECS from a glass micropipette and repeatedly recording the resulting diffusion cloud with a charge-coupled device (CCD) camera. Because the camera observes an image formed by a microscope, the optical properties of the imaging system (its point-spread function) must be taken into account.

2. Theory

We shall investigate concentration $c(\vec{r}, t)$ of some extracellular marker as a function of position in space $\vec{r} = (x_1, x_2, x_3)$ and time t. In a geometrically complex ECS, all the diffusion parameters are defined as volume-averaged local quantities over a sufficiently large sampling volume. The concentration is related to the tissue volume rather than the ECS volume because the optical method does not distinguish between the tissue compartments. We assume that a homogeneous but anisotropic environment with time-dependent diffusion characteristics can be described by an effective diffusion tensor

$$D_{ij}^{\star}(t) = D\Theta_{ij} \,, \tag{1}$$

where D is the scalar free diffusion constant and Θ_{ij} is the diffusion permeability tensor. Both indices run from 1 to 3. In an environment where the loss of diffusing substance is proportional to the concentration, we also introduce linear time-dependent clearance $\kappa(t)$, which is also assumed to be homogeneous. The diffusion equation in this environment is

$$\frac{\partial c(\vec{r}, t)}{\partial t} = D_{ij}^{\star}(t)\frac{\partial^2 c(\vec{r}, t)}{\partial x_i \partial x_j} - \kappa(t)c(\vec{r}, t) \,, \tag{2}$$

where we used Einstein's notation for sums ($a_i b_i = \mathbf{a} \cdot \mathbf{b} = \sum_{i=1}^{3} a_i b_i$). Equation (2) expresses the mass preservation when the diffusion flow $\vec{j}$ obeys Fick's law

$$j_i(\vec{r}, t) = -D_{ik}(t)\frac{\partial c(\vec{r}, t)}{\partial x_k} \,.$$

The initial concentration at time t_0 is represented by a function $c(\vec{r}, t_0)$.

Equation (2) with its initial condition can be solved in the Fourier domain. Fourier transform of $c(\vec{r}, t)$ with respect to the three spatial coordinates is defined as

$$\hat{c}(\vec{k}, t) = \iiint_{-\infty}^{\infty} c(\vec{r}, t) \exp(2\pi i k_j x_j) \, d\vec{r},$$

and the inverse as

$$c(\vec{r}, t) = \iiint_{-\infty}^{\infty} \hat{c}(\vec{k}, t) \exp(-2\pi i k_j x_j) \, d\vec{k} \,.$$

The Fourier transform turns Eq. (2) into

$$\frac{\partial \hat{c}(\vec{k}, t)}{\partial t} = -\left(4\pi^2 k_i D_{ij}^\star(t) k_j + \kappa(t)\right) \hat{c}(\vec{k}, t) \tag{3}$$

with the initial condition $\hat{c}(\vec{k}, t_0)$.

Solving Eq. (3) with respect to time yields

$$\hat{c}(\vec{k}, t) = \hat{c}(\vec{k}, t_0)\hat{c}_\delta(\vec{k}, t) , \tag{4}$$

where

$$\hat{c}_\delta(\vec{k}, t) = Q_\delta(t) \exp\left(-2\pi^2 k_i \Sigma_{ij}(t) k_j\right) , \tag{5}$$

$$Q_\delta(t) = \exp\left(-\int_{t_0}^t \kappa(t') \, dt'\right) , \tag{6}$$

and

$$\Sigma_{ij}(t) = 2\int_{t_0}^t D_{ij}^\star(t') \, dt' . \tag{7}$$

When the initial condition is Dirac's δ-function $\delta(\vec{r})$, its Fourier transform is unity. The inverse Fourier transform $c_\delta(\vec{r}, t)$ of $\hat{c}_\delta(\vec{k}, t)$ therefore describes the diffusion cloud initiated by the point source at time $t = t_0$:

$$c_\delta(\vec{r}, t) = Q_\delta(t)\phi_\delta(\vec{r}, t) , \tag{8}$$

where

$$\phi_\delta(\vec{r}, t) = \frac{1}{(2\pi)^{\frac{3}{2}} \left[\det(\Sigma_{ij})\right]^{\frac{1}{2}}} \exp\left(-\frac{x_i \Sigma_{ij}^{-1}(t) x_j}{2}\right) . \tag{9}$$

This is a 3D Gaussian distribution with variance matrix $\Sigma_{ij}(t)$ and with the total amount of diffusing substance decreasing as $Q_\delta(t)$ from its initial value of $Q_\delta(t_0) = 1$.

Multiplication in the Fourier domain corresponds to a convolution in the spatial domain. The concentration distribution following an arbitrary initial condition can therefore be written as

$$c(\vec{r}, t) = \iiint_{-\infty}^\infty c(\vec{r}', t_0) c_\delta(\vec{r} - \vec{r}', t) \, d\vec{r}' . \tag{10}$$

The total amount of diffusing substance is initially $Q(t_0) = \iiint_{-\infty}^\infty c(\vec{r}, t_0) \, d\vec{r}$ and changes with time as

$$Q(t) = \iiint_{-\infty}^\infty c(\vec{r}, t) \, d\vec{r} = Q(t_0)Q_\delta(t) , \tag{11}$$

where $Q_\delta(t)$ is substituted from Eq. (6). If a 3D measurement of concentration in time is available, the clearance $\kappa(t)$ can be computed from Eq. (11):

$$\kappa(t) = -\frac{d}{dt} \ln\left(\frac{Q(t)}{Q(t_0)}\right) . \tag{12}$$

119

Since the substance loss is homogeneous in space, the effect of nonzero clearance simply amounts to a global scaling of amplitude.

If the measured 3D concentration is normalized by the total amount $Q(t)$ of the diffusing substance at every time, a probability density function

$$\phi(\vec{r}, t) = \frac{c(\vec{r}, t)}{Q(t)} \tag{13}$$

can be constructed and the tensor of its second moments $\mu_{ij}(t)$ computed:

$$
\begin{aligned}
\mu_{ij}(t) &= \iiint_{-\infty}^{\infty} x_i x_j \phi(\vec{r}, t)\, d\vec{r} \\
&= \frac{1}{Q(t_0)} \iiint_{-\infty}^{\infty} c(\vec{r}', t_0) \left[\iiint_{-\infty}^{\infty} x_i x_j \phi_\delta(\vec{r} - \vec{r}', t)\, d\vec{r} \right] d\vec{r}' \\
&= \frac{1}{Q(t_0)} \iiint_{-\infty}^{\infty} c(\vec{r}', t_0) \left[\Sigma_{ij}(t) + x_i' x_j' \right] d\vec{r}' \\
&= \Sigma_{ij}(t) + \mu_{ij}(t_0).
\end{aligned}
\tag{14}
$$

The components of the effective diffusion tensor are now easily extracted as time derivatives of these moments:

$$D_{ij}^{\star}(t) = \frac{1}{2} \frac{d\mu_{ij}(t)}{dt}. \tag{15}$$

Unfortunately, a complete 3D measurement of the concentration is not usually available. More common is an experimental setup with a traditional (non-confocal) microscope where a 2D image is recorded. Because the microscope's objective has a finite aperture, the system appears to be imaging a virtual object, constructed from the true object by a convolution with the point-spread function (PSF) $S(\vec{r})$ of the system. The effective width of the PSF limits the system resolution. Using the approximation for $S(\vec{r})$ suggested by [3], we can derive estimates for the effective "horizontal" and "vertical" resolutions Δ_h and Δ_v, respectively:

$$\Delta_h = 0.61\lambda \frac{\sqrt{n^2 - N_A^2}}{n N_A} \quad \text{and} \quad \Delta_v = 2\lambda \frac{n^2 - N_A^2}{n N_A^2}, \tag{16}$$

where λ is the wavelength, n is the index of refraction of the environment under the objective, and N_A is the numerical aperture. The horizontal resolution is typically smaller than the corresponding size of the recorded image pixel and the horizontal PSF effect can thus be safely ignored. Resolution Δ_v along the microscope optical axis is usually much lower and cannot be ignored. Under these assumptions, we can utilize the PSF approximation in the object space

$$S(\vec{r}) = \delta(x_1)\delta(x_2) S_v(x_3), \tag{17}$$

where

$$S_v(x_3) = \frac{1}{\Delta_v} \operatorname{sinc}^2\left(\frac{\pi x_3}{\Delta_v}\right) \tag{18}$$

and $\operatorname{sinc}(x) = \sin(x)/x$. We shall see that the exact functional form of $S_v(x_3)$ is not important but the validity of the approximation given by Eq. (17) is.

If the PSF was very sharp $(S(\vec{r}) = \delta(\vec{r}))$, the imaging system would simply record 2D image proportional to the concentrations $c(x_1, x_2, x_3 = z_0, t)$ in the plane of focus $x_3 = z_0$. Due to the PSF blurring effect, however, it instead appears to detect signal originating from concentration

$$
\begin{aligned}
c_s(x_1, x_2, z_0, t) &= \iiint_{-\infty}^{\infty} c(\vec{r}', t) S(\vec{r} - \vec{r}') \, d\vec{r}' \\
&= \int_{-\infty}^{\infty} c(x_1, x_2, x_3', t_0) S_v(z_0 - x_3') \, dx_3' \\
&= \iiint_{-\infty}^{\infty} c_\delta(\vec{r}', t) \int_{-\infty}^{\infty} c(x_1 - x_1', x_2 - x_2', \xi, t_0) S_v(z_0 - x_3' - \xi) \, d\xi \, d\vec{r}' \\
&= \iiint_{-\infty}^{\infty} c_\delta(\vec{r}', t) c_s(x_1 - x_1', x_2 - x_2', z_0 - x_3', t_0) \, d\vec{r}' \, .
\end{aligned}
\tag{19}
$$

It can be seen that the effect of microscope's PSF in our approximation results in a simple modification (blurring along the x_3 axis) of the initial condition $c(\vec{r}, t_0)$ to $c_s(\vec{r}, t_0)$. After this modification, we can consider the microscope to perfectly follow the rules of geometrical optics, magnifying the image by a constant factor M and amplifying the image signal by another constant factor A. A single in-focus plane $x_3 = z_0$ through c_s is imaged.

Assuming that a 2D section at $x_3 = z_0$ of the concentration cloud elicited by the initial condition $c_s(\vec{r}, t_0)$ represents all the information that is available to us, let us extract as much as possible from it. The image intensity $I(x_1, x_2, t)$ expressed in the object coordinates after constant amplification A is

$$I(x_1, x_2, t) = A c_s(x_1, x_2, z_0, t) \, . \tag{20}$$

For the integrated total image intensity $Q_I(t)$ we get

$$
\begin{aligned}
Q_I(t) &= \iint_{-\infty}^{\infty} I(x_1, x_2, t) \, dx_1 \, dx_2 \\
&= A Q_\delta(t) \iiint_{-\infty}^{\infty} c_s(\vec{r}', t_0) \phi_{\delta v}(z_0 - x_3', \Sigma_{33}) \, d\vec{r}' \, ,
\end{aligned}
\tag{21}
$$

where

$$\phi_{\delta v}(\xi, \Sigma_{33}) = \frac{1}{\sqrt{2\pi\Sigma_{33}}} \exp\left(-\frac{\xi^2}{2\Sigma_{33}}\right) \tag{22}$$

is the "vertical" portion of the Gaussian distribution ϕ_δ. We have made the dependency on $\Sigma_{33} = \Sigma_{33}(t)$ explicit to emphasize it. In contrast to the 3D measurement, the time dependency is not fully determined by the clearance term $Q_\delta(t)$.

Finally, let us calculate the second moment $\mu_{JK}(t)$ of the image. Capitalized indices are introduced to distinguish their 2D range ($J, K = 1, 2$).

$$
\begin{aligned}
\mu_{JK}(t) &= \frac{1}{Q_I(t)} \iint_{-\infty}^{\infty} x_J x_K I(x_1, x_2, t) \, dx_1 \, dx_2 \\
&= \frac{A Q_\delta(t)}{Q_I(t)} \iiint_{-\infty}^{\infty} c_s(\vec{r}', t_0) \left[\iint_{-\infty}^{\infty} x_J x_K \phi_\delta(\vec{r} - \vec{r}', t) \, dx_1 \, dx_2 \right] d\vec{r}' .
\end{aligned}
\tag{23}
$$

In the general anisotropic case with an arbitrarily rotated coordinate system, the result is rather complicated. However, it is usually possible to make one of the principle axes parallel to the x_3 axis of the imaging system. We then have

$$
\Sigma_{ij}(t) = \begin{pmatrix} \Sigma_{11}(t) & \Sigma_{12}(t) & 0 \\ \Sigma_{21}(t) & \Sigma_{22}(t) & 0 \\ 0 & 0 & \Sigma_{33}(t) \end{pmatrix} .
$$

This finally leads to

$$
\mu_{JK}(t) = \Sigma_{JK}(t) + \frac{\iiint_{-\infty}^{\infty} x_J x_K c_s(\vec{r}, t_0) \phi_{\delta v}(z_0 - x_3, \Sigma_{33}(t)) \, d\vec{r}}{\iiint_{-\infty}^{\infty} c_s(\vec{r}, t_0) \phi_{\delta v}(z_0 - x_3, \Sigma_{33}(t)) \, d\vec{r}} .
\tag{24}
$$

3. Discussion

In Eq. (24), we have obtained a result useful for a biologist employing the FOTOD modification of the IOI method. It provides a means of extracting the effective diffusion coefficient as a function of time.

The experimentally accessible quantity is $\mu_{JK}(t)$. However, its time derivative yields the corresponding components of the diffusion tensor D_{JK} only if the last term of Eq. (24) is constant in time. Its time dependency is determined by the shape of the initial condition. When the initial condition is separable in the variable x_3, the blurred initial condition will also be separable, and the time dependency of this term will "cancel out". Therefore, for a commonly assumed Gaussian initial condition, which is obviously separable, the extraction of the diffusion tensor is straightforward. For a more realistic spherical initial condition though, the experimental curve of variance versus time will not be linear even when the diffusion tensor is constant in time.

Acknowledgments

References

[1] Hrabě, J., Hrabětová, S., and Segeth, K.: A model of effective diffusion and tortuosity in the extracellular space of the brain. Biophys. J. **87** (2004), 1606–1617.

[2] Hrabětová, S. and Nicholson, C.: *Eletrochemical methods for neuroscience*. CRC, Boca Raton, Florida, 2007.

[3] Nicholson, C. and Tao, L.: Hindered diffusion of high molecular weight compounds in brain extracellular microenvironment measured with integrative optical imaging. Biophys. J. **65** (1993), 2277–2290.

[4] Syková, E. and Nicholson, C.: Diffusion in brain extracellular space. Physiol. Rev. **88** (2008), 1277–1340.